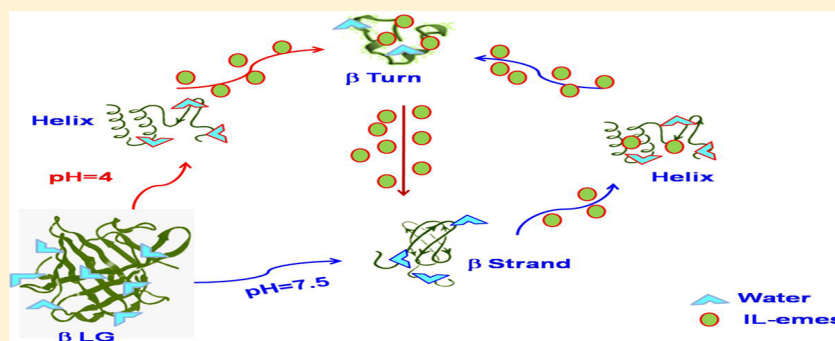


# Microviscosity-Induced Conformational Transition in $\beta$ -Lactoglobulin in the Presence of an Ionic Liquid

Kamatchi Sankaranarayanan,<sup>†</sup> B. Sreedhar,<sup>‡</sup> B.U. Nair,<sup>†</sup> and A. Dhathathreyan<sup>†,\*</sup>

<sup>†</sup>Chemical Laboratory, CSIR-CLRI, Adyar, Chennai 600020, India

<sup>‡</sup>Inorganic and Physical Chemistry Division, CSIR-Indian Institute of Chemical Technology, Hyderabad 500 607, India



**ABSTRACT:** This study reports on the helix–beta conformation transition of bovine  $\beta$ -lactoglobulin ( $\beta$ LG) prepared at two different pH conditions (pH 4 and 7.5) and in the presence of the ionic liquid 1-ethyl-3-methylimidazolium ethyl sulfate (IL-emes). The investigation was carried out by combining a range of techniques such as circular dichroic (CD) spectroscopy, steady-state fluorescence spectroscopy, isothermal titration calorimetry (ITC), and transmission electron microscopy. The influence of microviscosity induced by IL-emes on the secondary structure of  $\beta$ LG was studied using a quartz crystal microbalance and correlated with the steady-state fluorescence emission. The effect of heat on the helix–beta transition in  $\beta$ LG was directly measured by ITC by titrating  $\beta$ LG with IL-emes. The net effect of heat after subtraction of the heat of dilution was negative in both cases, suggesting that the protein moves to a stable conformation. The changes in the overall aggregated structures were confirmed by transmission electron microscopy, where a shift in the size and morphology of aggregates was found, from large clusters (size of 70 nm) at pH 4 to smaller aggregates (size of 20 nm) at pH 7.5, which reduced to 7 nm in the presence of the IL. The transformation of helical to beta structure at pH 4 show that the folding pathway in the presence of the ionic liquid is hierarchical, whereas at neutral pH, it appeared to be nonhierarchical and the final native structure was acquired by nonlocal interactions through typical forces involved in the stabilization of the tertiary structure.

## INTRODUCTION

Proteins play important roles in biological functions and carry out most of the important tasks in living cells. For them to perform these important tasks, their folding patterns in three dimensions are important. Throughout the folding process, a protein is expected to have some amount of conformational stability. The energy differences between the various folded states are on the order of 5–15 kcal/mol. This very small energy difference between the states makes industrial or pharmaceutical applications of certain proteins difficult, especially when the protein is subjected to extremes of temperature and pH or dissolved in destabilizing agents such as organic solvents. There is presently a great deal of interest in developing methodologies to increase the conformational stability of proteins. Although many methods are available, it is still difficult to stabilize proteins efficiently and effectively.<sup>1–4</sup> Misfolding of a protein leading to fibrillation under certain conditions of solvation was reported by Guijarro et al.<sup>5</sup> In recent times, research has focused on understanding the aggregated structures of peptides and proteins, especially from

the points of view of both functional and aberrant phenomena in nature, ranging from the formation of actin filaments to pathological aggregation of these peptide and protein molecules into amyloid fibrils.<sup>6</sup>

Most of these fibrils share a common cross- $\beta$ -sheet structure and seem to be associated with a range of increasingly prevalent clinical disorders, including Alzheimer's and Parkinson's diseases.<sup>7–10</sup> Recent research on the coordination of metal ions with amyloid fibrils showed that metal ions can induce aggregation of proteins and modulate the fibrillation process.<sup>11–13</sup>

In this work, microviscosity-induced conformational transitions in  $\beta$ -lactoglobulin ( $\beta$ LG) in the presence of the ionic liquid 1-ethyl-3-methylimidazolium ethyl sulfate (IL-emes) were studied.  $\beta$ LG, which is found in the milk of several mammalian species, is similar to the hydrophobic carrier-

**Received:** October 16, 2012

**Revised:** January 11, 2013

**Published:** January 15, 2013

retinol-binding protein<sup>14</sup> and bilin-binding protein<sup>15</sup> and shows a three-dimensional structural pattern termed the  $\beta$ -barrel.<sup>16,17</sup>

Depending on pH, temperature, and concentration,  $\beta$ LG exists in various oligomeric states,<sup>18,19</sup> and some additives induce conformational changes in it.<sup>20–23</sup> Below pH 3.0,  $\beta$ LG is mainly monomeric, whereas at neutral pH, it is mainly dimeric.

It is known that ionic liquids, with properties such as nonvolatility, thermal stability, low melting temperature, high decomposition temperature, low viscosity, and zero toxicity, are ideal choices for regulating the organization of hydrated peptides or proteins.<sup>24–30</sup> A number of studies have reported on the influence of ILs on the organization and activity of proteins and enzymes.<sup>31–37</sup>

In the present work, changes in the aggregation and organized assemblies of  $\beta$ LG in the presence of IL-emes, at pH values below and above the isoelectric point (pI) of the protein, were analyzed. The microviscosity of the samples measured using a quartz crystal microbalance (QCM) was correlated with the structural changes of  $\beta$ LG using UV–visible, fluorescence, and circular dichroism (CD) spectroscopic techniques. In addition, isothermal titration calorimetry (ITC) was used to monitor the thermodynamic parameters associated with the protein–IL interactions and ensuing conformational changes.

Studies of  $\beta$ LG conformations have focused on the relevance of the central hydrophobic cavity in the binding of amphiphilic molecules, thus determining its functions.<sup>38</sup> Amyloid fibril formation in  $\beta$ LG promoted by the denaturant urea was reported by Hamada and Dobson.<sup>39</sup>

Giurleo et al. proposed a three-step process by which monomers of  $\beta$ LG are converted first into weakly associated aggregates, which then rearrange into stable aggregates that eventually convert into longer protofibrils.<sup>40</sup>

An important step forward in understanding the role of protein molecular structure in the toxicity of amyloid fibrils in diseases involving protein misfolding was postulated by van den Akker et al. Using combined AFM imaging and vibrational sum frequency generation spectroscopy in  $\beta$ LG, they showed that the  $\beta$ -sheet content influences the amyloid nanofibril rigidity.<sup>41</sup>

## EXPERIMENTAL SECTION

$\beta$ LG from bovine milk and the ionic liquid 1-ethyl-3-methylimidazolium ethyl sulfate (IL-emes) were purchased from Sigma-Aldrich (St. Louis, MO) and were more than 99% pure. All aqueous solutions were prepared with distilled water further purified with a four-stage Milli-Q water system (resistivity greater than 18.2 M $\Omega$ ; Millipore, Billerica, MA). Solutions of  $\beta$ LG were prepared at pH 4.0 (using 10 mM acetate buffer) and pH 7.5 (using 10 mM phosphate buffer).  $\beta$ LG (10 and 1  $\mu$ M) at pH 4 or 7.5 was dissolved in various concentrations of hydrated IL-emes (from 0.05 to 10 mM), and the mixtures were stirred in a magnetic stirrer overnight to avoid any phase separation. The resulting solutions were clear and were used for all of the experiments. The pH of the protein with IL-emes at the different concentrations was checked and found to be the same as that of the corresponding solution of pure protein.

**UV–Visible and Fluorescence Spectroscopies.**  $\beta$ LG and  $\beta$ LG + IL-emes samples were analyzed using a UV-1800 Shimadzu spectrophotometer with quartz cells of 1-cm path length. The corresponding hydrated IL-emes was used as a reference for the measurements. Steady-state fluorescence

spectroscopy was performed using a Cary Eclipse spectrometer with  $\lambda_{\text{ex}} = 280$  nm.

**QCM Measurements.** Plasma-cleaned (exposed to UV/ozone for 10 min) gold-coated quartz substrates were used for all QCM measurements. Measurements were performed with 50  $\mu$ L of temperature-stabilized and degassed sample liquid, which was delivered to the chamber containing the sensor crystal to ensure the complete exchange of the liquid. This ensured that processes of adsorption and surface adlayer changes could be followed in situ while subsequently exposing different solutions to the surface. All measurements were performed at a temperature of 24–25  $^{\circ}$ C. QCM sensors, crystal holders, and polished gold AT-cut 5 MHz gold crystals of 25-mm-diameter crystals from Maxtek were used for the study. The oscillation frequency was measured using a Maxtek research QCM (RQCM) with phase-lock oscillator with independent crystal measurement channel. Data acquisition was performed using the Maxtek RQCM Data Logging software (v. 1.6.0) on a PC connected through an RS-232 serial interface. A sampling rate of 1/60 Hz was employed for all experiments. Any baseline drift was regulated using the coarse and fine capacitance adjustments. Upon interaction of the protein with the surface of a sensor crystal, changes in the resonance frequency,  $\Delta f$ , related to the attached mass are governed by the Sauerbrey equation

$$\Delta m = -\frac{(\mu\rho)^{1/2}\Delta f}{2f_0^2} \quad (1)$$

where  $f_0$  is the resonance frequency of the crystal (5 MHz at 25  $^{\circ}$ C),  $\mu$  is the shear modulus of the quartz crystal ( $2.947 \times 10^{11}$  g s $^{-2}$  cm $^{-1}$  at room temperature), and  $\rho$  is the density of quartz (2.648 g cm $^{-3}$ ).

Shear viscosity is then given by the equation

$$\eta = [19.627 \times 10^{-7}(\Delta f)^2]/\rho \quad (2)$$

**CD Spectroscopy.** CD spectra of  $\beta$ LG (at pH 4 and 7.5) pure and with IL-emes were obtained using a JASCO J-715 spectropolarimeter (JASCO Corp., Tokyo, Japan). Far-UV (240–190 nm) spectra of the protein in different levels of hydrated IL were obtained using 0.1-cm-path-length quartz cells and were analyzed using the Dichroweb fitting to three structural parameters:  $\alpha$ -helix,  $\beta$ -sheet, and aperiodic.<sup>42</sup> In another experiment, the same solutions were aged for 1 week by being stored under controlled conditions of temperature and humidity, after which CD measurements were repeated.

**Isothermal Titration Calorimetry (ITC).** Titration microcalorimetry was performed on a nanowatt-scale isothermal titration microcalorimeter supported by a TAM III thermal activity monitor (TA Instruments, Söllerntuna, Sweden). For the measurement of the protein ( $\beta$ LG)/IL-emes solutions, the 3-mL sample cell of the calorimeter made from stainless steel was initially loaded with 2700  $\mu$ L of the  $\beta$ LG solution whose concentration was 10  $\mu$ M. Then, 0.1 M IL-emes solution was injected into the stirred sample cell at 90 rpm in 2- $\mu$ L additions using a 500- $\mu$ L Hamilton syringe controlled by a TA 3810 syringe pump. The interval between two injections was 20 min, which was sufficiently long for the signal to return to the baseline. All experiments were performed at a fixed temperature of  $298.15 \pm 0.01$  K and repeated thrice. To deduct the heats of dilution of the ionic liquid and  $\beta$ LG solutions, titration experiments of ionic liquid solution into buffer solution and  $\beta$ LG solution into buffer solution were performed.

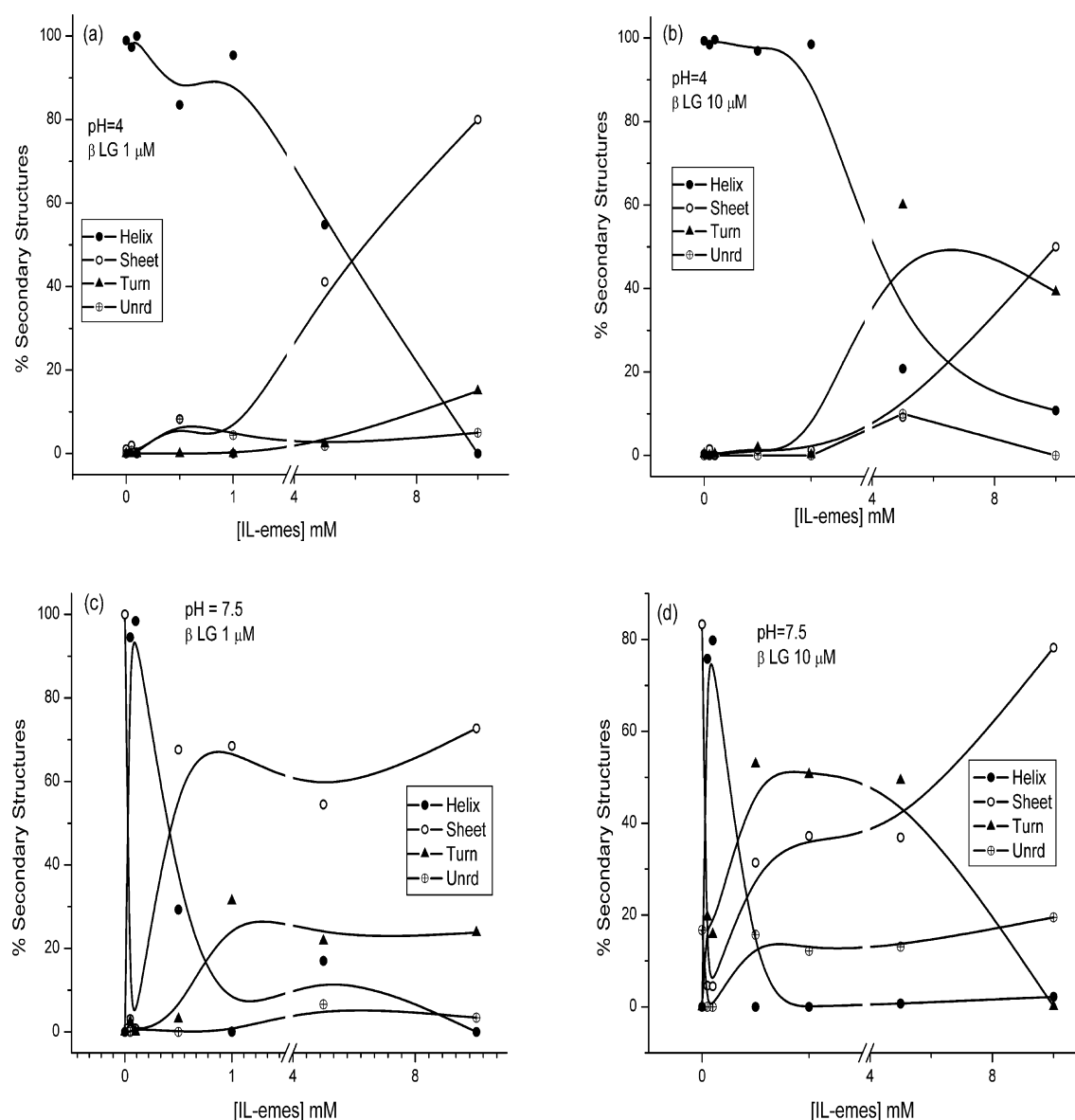


**Figure 1.** Secondary structure percentages of  $\beta$ LG at pH (a,b) 4 and (c,d) 7.5 for concentrations of (a,c) 1 and (b,d) 10  $\mu$ M. (Connecting lines are only a guide to the eyes.)

**Transmission Electron Microscopy (TEM).** TEM studies were carried out by dipcoating  $\beta$ LG solutions on Formvar/carbon-coated copper grids (200 mesh size) using a TECNAI FE12 TEM instrument operating at 120 kV. The images were viewed by SIS imaging software.

## RESULTS AND DISCUSSION

The UV–visible spectra of  $\beta$ LG at two concentrations (1 and 10  $\mu$ M) and at pH 4 and 7.5 showed that, for increasing concentrations of IL, the absorbance did not change dramatically, suggesting that there were no changes in the ground-state properties of the protein due to the presence of the ionic liquid.

The secondary structural changes of these samples were evaluated using CD spectroscopy. Figure 1a,b shows the percentage populations of different secondary structures of  $\beta$ LG at two concentrations (1 and 10  $\mu$ M) and at pH 4 for varying concentrations of IL. At this pH, the pure protein showed a high percentage of helicity compared with the sheet

structure. This high non-native helical content is a well-established conformational state for  $\beta$ LG at low pH.<sup>43</sup> Using the hierarchical model for  $\beta$ -sheet proteins,<sup>44</sup> the possibility of a high percentage of non-native  $\alpha$ -helix intermediates being accumulated in the folding pathway of predominantly  $\beta$ -sheet proteins, such as  $\beta$ LG, has been suggested.<sup>45,46</sup>

As the concentration of ionic liquid increased, the protein initially shifted to a  $\beta$ -turn structure, which then converted to almost 50%  $\beta$ -sheet. Usually,  $\beta$ -turns are reported as intermediate states<sup>47</sup> that allow the protein to flip-flop between helical and sheet-like structures. This stepwise conversion of the helical conformation to a  $\beta$ -turn and finally to a  $\beta$ -sheet could be due to changes in the rates of folding of the protein due to an increase in local viscosity and seemed to take place sequentially.

At pH 7.5,  $\beta$ LG is known to have a major percentage of  $\beta$ -sheet in the secondary structure. Figure 1c,d shows the % secondary structures of  $\beta$ LG with two concentrations (1 and 10  $\mu$ M) at this pH in the presence of IL. Here, except for a small

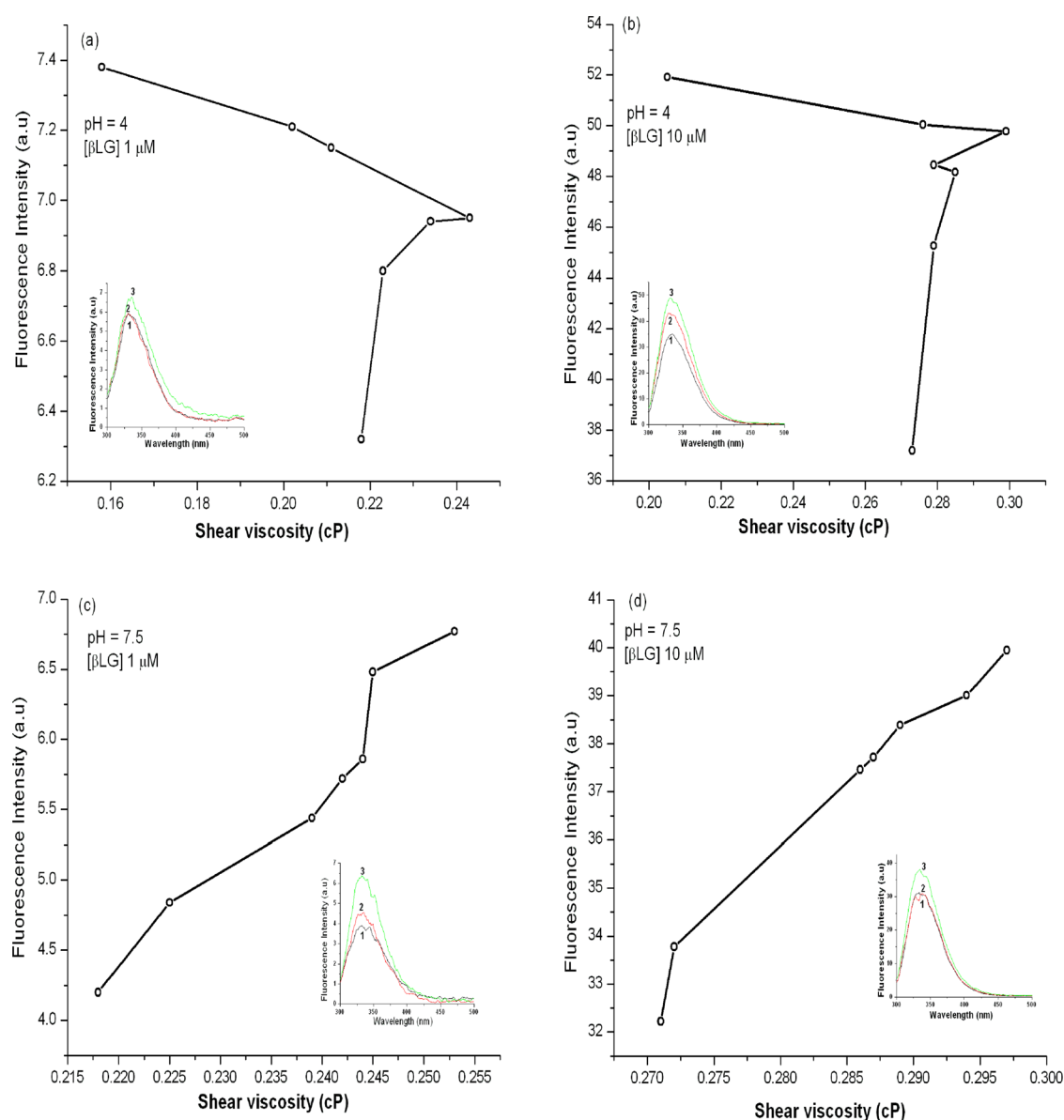


**Figure 2.** Shear viscosity versus steady-state fluorescence intensity at pH (a,b) 4 and (c,d) 7.5 for  $\beta$ LG concentrations of (a,c) 1 and (b,d) 10  $\mu\text{M}$ . Inset: Steady-state fluorescence spectra of (1) pure  $\beta$ LG, (2)  $\beta$ LG + 0.05 mM IL-emes, and (3)  $\beta$ LG + 10 mM IL-emes.

range at low concentrations of IL where the  $\beta$ LG initially underwent a transition to helix, the protein remained in the  $\beta$ -sheet structure with increasing concentrations of IL.

On aging of the samples (for about a week), the protein showed a complete transition to the  $\beta$ -sheet structure. Using QCM, for the two concentrations of  $\beta$ LG, shear viscosity was estimated for increasing concentrations of IL.

Figure 2 shows the change in fluorescence against shear viscosity for  $\beta$ LG at pH 4 and 7.5. Here the emission from the Trp residue in the protein was monitored for the changing environment. From the plots, it can be seen that, at pH 4, the transition to the  $\beta$ -sheet structure led to a dramatic drop in viscosity, which was also reflected in the lowering of the emission intensity. On the other hand, at pH 7.5, there was an increase in intensity for increasing viscosity of the protein. This suggests that the change in the microviscosity and any molecular crowding experienced by  $\beta$ LG due to the presence of the IL was better expressed in the Trp emission at higher pH. At pH 4, the emission properties did not seem to be very

sensitive to the medium viscosity, because of possible shielding and isolation of the Trp from the surroundings.

For the ITC and TEM studies, a protein concentration of 10  $\mu\text{M}$  was chosen. ITC was used in this study to analyze the interaction of the ionic liquid with the protein during the titration of  $\beta$ LG against the concentration of IL-emes. As control experiments, titrations of the ionic liquid into buffer solution and the  $\beta$ LG solution into buffer solution did not show any large changes in heat flow.

Enthalpy variations (i.e., gains or losses) were calculated as the heat released per mole of injected IL and were attributed to the different molecular events, for example, types of binding, protein unfolding, or protein aggregation. However, assigning the enthalpy to any particular event is not easy because the final measured signal has contributions from many different physicochemical phenomena and conformational changes.

Figure 3a shows a plot of ITC raw data for various additions of ionic liquid to the protein solution, and Figure 3b shows the integrated normalized heat per mole of the injectant plotted

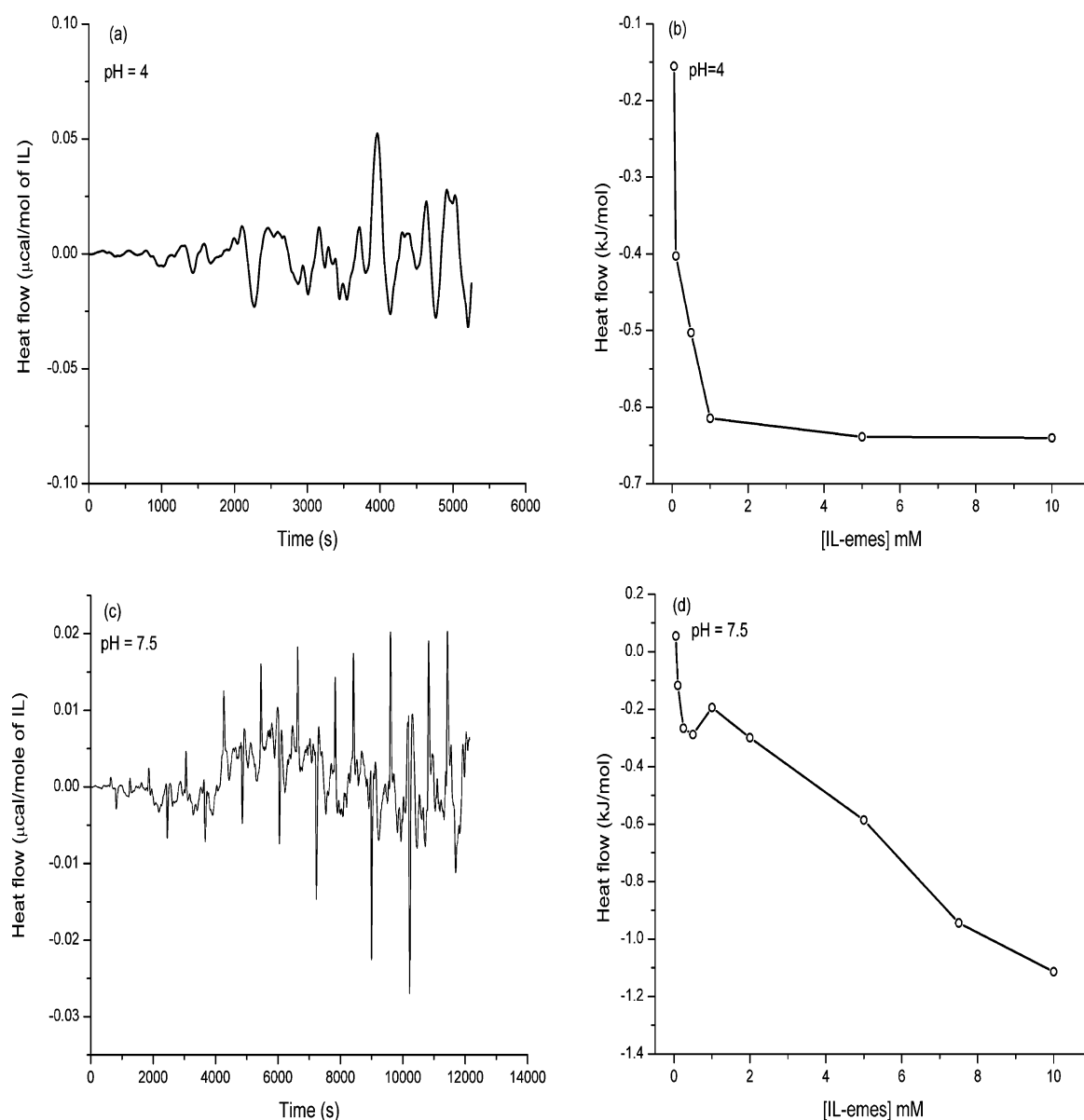


**Figure 3.** (a,c) Heat flow as a function of time for various additions of ionic liquid to the protein solution at pH (a) 4 and (c) 7.5. (b,d) Integrated normalized heat per mole of the injectant plotted against the IL concentration in the cell at pH (b) 4 and (d) 7.5.

against the IL concentration in the cell at pH 4. The plots clearly demonstrate that the ionic-liquid-driven assembly of the protein involved favorable (negative) enthalpy changes and favorable entropy changes. Figure 3c shows a plot of the ITC raw data for the addition of ionic liquid to the protein solution, and Figure 3d shows the integrated normalized heat per mole of the injectant plotted against the IL concentration in the cell at for different concentrations of IL at pH 7.5. Both of the plots show two steps, and the enthalpy is more negative at pH 7.5 than at pH 4.

In general, for a protein–protein interaction, the enthalpy of association ( $\Delta H_A$ ) is contributed by three major terms: (i) conformational enthalpy that arises due to the formation of an ordered secondary structure; (ii) interaction enthalpy that arises due to hydrogen bonding, van der Waals forces, and electrostatic forces; and (iii) solvation (hydration/dehydration) enthalpy that arises due to the removal or intake of water molecules at the interface.

The surface activity of organized assemblies of  $\beta$ LG at the air/water interface have shown that the protein is more surface-active at pH 4 than at pH 7.5, suggesting that the contribution from solvation and the interaction enthalpy is higher at pH 4.<sup>48</sup> On the other hand, at pH 7.5, the major contribution to the enthalpy is mainly from the conformational change, as evidenced from CD spectral studies. Typically, in most protein–small molecule interaction studies using ITC, a binding constant is estimated. However, in the present study, such a binding constant was not reported here because the system was slightly more complicated than just a protein–IL interaction. Here, the ternary interactions of water–IL, IL–protein, and protein–water all play a role and need not necessarily be additive. Hence, a rigorous model based on Molecular Dynamic Simulation (MDS) needs to be carried out to study this aspect and work is presently underway.

The effects of pH and change in the local viscosity on the appearance of  $\beta$ LG dispersions are shown in the TEM micrographs presented in Figure 4. Here, no staining agents



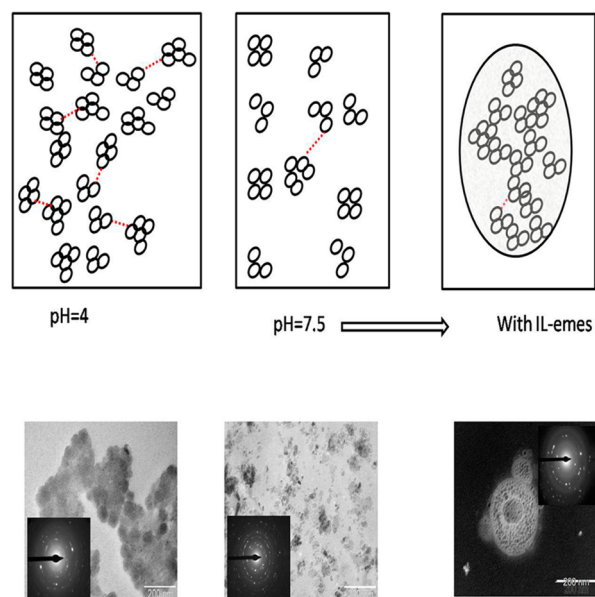


**Figure 4.** Transmission electron micrographs and schematic representation of  $\beta$ LG at pH 4 and 7.5 and with IL-emes.

were used, and the sizes of the aggregates ranged from 70 nm (at pH 4) to 22 nm (pH 7.5). In the presence of the ionic liquid, spherical particles (individual particle sizes of about 7–8 nm) that aggregated together were seen. This could arise from the increase in local viscosity, leading to a slowing of the particles, which then formed these large aggregates.

A schematic diagram of the formation of different-sized structures at pH 4 and 7.5 and at pH 7.5 with ionic liquid is given in Figure 4. It is known that  $\beta$ LG in the pH range of 3.7–5.2 forms a larger oligomer<sup>49</sup> with a maximum self-association at around pH 4.6, which suggests involvement of specific interactions. Based on this fact, it is possible that such oligomeric species at pH 4 form the large-sized cluster (as seen by TEM). Under physiological conditions (neutral pH and  $\beta$ LG concentration > 50  $\mu$ M),  $\beta$ LG is predominantly dimeric. In the present work, the highest concentration of  $\beta$ LG was 10  $\mu$ M, which was well below the 50  $\mu$ M limit suggested by Gottschalk et al.<sup>50</sup> Thus, predominantly monomeric species were involved at pH 7.5. Such monomeric species are likely to interact through disulfide bridges and possibly form smaller clusters, as seen in the TEM micrographs. At pH 7.5, the protein is expected to be negatively charged. As the microviscosity increased in the presence of IL, clusters of clusters would form due to partial screening of the charged clusters by the IL.

## CONCLUSIONS

This study shows that a traditionally beta protein such as  $\beta$ LG can undergo conformational transitions to the non-native helical form and revert back to its native beta state as a result changes in microviscosity arising from the presence of an ionic liquid. The influence of the microviscosity on the protein is pronounced at pH 7.5.

The CD spectral data showed that the secondary structure changes in the protein induced by IL-emes cannot be explained by a simple  $\beta$ -sheet–helix transition.

In the presence of ionic liquid, at pH 4, the initial helical structure of the protein transformed into an intermediate  $\beta$ -turn structure that then changed to the more stable native  $\beta$ -sheet structure, indicating the hierarchical nature of the

transformation. At pH 7.5, the initial native beta state traversed to a helical structure and then returned to the native beta state in the presence of IL-emes. This is very similar to the overshoot phenomenon in  $\beta$ LG with trifluoroethanol observed by Mendieta et al.<sup>51</sup> At pH 7.5, the role of microviscosity in determining the folding pattern of the protein was dominant, showing that nonspecific interactions play an important role here.

In summary, at acidic pH, the folding pathway in the presence of the ionic liquid is hierarchical, whereas at neutral pH, it appears to be nonhierarchical and the final native structure is acquired through nonlocal interactions that are typically involved in the stabilization of the tertiary structure.

## AUTHOR INFORMATION

### Corresponding Author

\*E-mail aruna@clri.res.in. Tel.: +91-44-24437167. Fax +91-44-24911589.

### Notes

The authors declare no competing financial interest.

## ACKNOWLEDGMENTS

The authors thank DST, Government of India, for a project grant (DST/TSG/ME/2011/51-G) under which part of this work was carried out. The authors acknowledge the assistance rendered by the late Mr. F. Chandrasekar, Technical Officer, CSIR-CLRI, in the ITC measurements. K.S. thanks CSIR, Government of India, for the award of a research fellowship.

## REFERENCES

- (1) Imoto, T. *Cell. Mol. Life Sci.* **1997**, *53*, 215–223.
- (2) Pace, C. N.; Shirley, B. A.; McNutt, M.; Gajiwala, K. *FASEB J.* **1996**, *10*, 75–83.
- (3) Pace, C. N. *Trends Biochem. Sci.* **1990**, *15*, 14–17.
- (4) Lehmann, M.; Wyss, M. *Curr. Opin. Biotechnol.* **2001**, *12*, 371–375.
- (5) Gujjarro, J. I.; Sunde, M.; Jones, J. A.; Campbell, I. D.; Dobson, C. M. *Proc. Natl. Acad. Sci. U.S.A.* **1998**, *95*, 4224–4228.
- (6) Frieden, C.; Goddette, D. W. *Biochemistry* **1983**, *22*, 5836–5843.
- (7) Hamley, I. W. *Angew. Chem., Int. Ed.* **2007**, *46*, 8128–8147.
- (8) Makin, O. S.; Atkins, E.; Sikorski, P.; Johansson, J.; Serpell, L. C. *Proc. Natl. Acad. Sci. U.S.A.* **2005**, *102*, 315–320.
- (9) Ross, C. A.; Poirier, M. A. *Nat. Rev. Mol. Cell Biol.* **2005**, *6*, 891–898.
- (10) Chimon, S.; Shaibat, M. A.; Jones, C. R.; Calero, D. C.; Aizezi, B.; Ishii, Y. *Nat. Struct. Mol.* **2007**, *14*, 1157–1164.
- (11) Pandey, N. K.; Ghosh, S.; Dasgupta, S. *J. Phys. Chem. B* **2010**, *114*, 10228–10233.
- (12) Uversky, V. N.; Li, J.; Fink, A. L. *J. Biol. Chem.* **2001**, *276*, 44284–44296.
- (13) Pal, P.; Mahato, M.; Kamilya, T.; Tah, B.; Sarkar, R.; Talapatra, G. B. *J. Phys. Chem. B* **2011**, *115*, 4259–4265.
- (14) Newcomer, M. E.; Jones, T. A.; Aqvist, J.; Sundelin, J.; Eriksson, U.; Rask, L.; Peterson, P. *EMBO J.* **1984**, *3*, 1451–1454.
- (15) Huber, R.; Schneider, M.; Epp, O.; Mayr, I.; Messerschmidt, A.; Pflugrath, J.; Kayser, H. *J. Mol. Biol.* **1987**, *195*, 423–434.
- (16) Papiz, M. Z.; Sawyer, L.; Eliopoulos, E. E.; North, A. C. T.; Findlay, J. B. C.; Sivaprasadarao, R.; Jones, T. A.; Newcomer, M. E.; Kraulis, P. J. *Nature* **1986**, *324*, 383–385.
- (17) Monaco, H. L.; Zanotti, G.; Spadon, P.; Bolognesi, M.; Sawyer, L.; Eliopoulos, E. E. *J. Mol. Biol.* **1987**, *197*, 695–706.
- (18) Timasheff, S. N.; Townsend, R. *Nature* **1964**, *203*, 517–519.
- (19) Zimmerman, K. D.; Barlow, G. H.; Klotz, I. M. *Arch. Biochem. Biophys.* **1970**, *138*, 101–109.
- (20) Coke, M.; Wilde, P. J.; Russell, E.; Clark, D. J. *Colloid Interface Sci.* **1990**, *138*, 489–504.

- (21) Dufour, E.; Haertlé, T. *Biochim. Biophys. Acta* **1991**, *1079*, 316–320.
- (22) Dufour, E.; Roger, P.; Haertlé, T. *J. Protein Chem.* **1992**, *11*, 645–652.
- (23) Dodin, G.; Andrieux, M.; Kabbani, H. *Eur. J. Biochem.* **1990**, *193*, 697–700.
- (24) Sankaranarayanan, K.; Dhathathreyan, A.; Krägel, J.; Miller, R. J. *Phys. Chem. B* **2012**, *116*, 895–902.
- (25) Sankaranarayanan, K.; Sathiyaraj, G.; Nair, B. U.; Dhathathreyan, A. *J. Phys. Chem. B* **2012**, *116*, 4175–4180.
- (26) Kowacz, M.; Mukhopadhyay, A.; Carvalho, A. L.; Esperanca, J. M. S. S.; Romão, M. J.; Rebelo, L. P. N. *Cryst. Eng. Commun.* **2012**, *14*, 4912–4921.
- (27) Akdogan, Y.; Junk, M. J. N.; Hinderberger, D. *Biomacromolecules* **2011**, *12*, 1072–1079.
- (28) Wei, W.; Danielson, N. D. *Biomacromolecules* **2011**, *12*, 290–297.
- (29) Attri, P.; Venkatesu, P. *Phys. Chem. Chem. Phys.* **2011**, *13*, 6566–6575.
- (30) Constantinescu, D.; Weingärtner, H.; Herrmann, C. *Angew. Chem., Int. Ed.* **2007**, *46*, 8887–8889.
- (31) Micaelo, N. M.; Soares, C. M. *J. Phys. Chem. B* **2008**, *112*, 2566–2572.
- (32) Rao, K. S.; Singh, T.; Trivedi, T. J.; Kumar, A. *J. Phys. Chem. B* **2011**, *115*, 13847–13853.
- (33) Danten, Y.; Cabac, M. I.; Besnard, M. *J. Phys. Chem. A* **2009**, *113*, 2873–2889.
- (34) van Rantwijk, F.; Sheldon, R. A. *Chem. Rev.* **2007**, *107*, 2757–2785.
- (35) Weingärtner, H.; Cabrele, C.; Herrmann, C. *Phys. Chem. Chem. Phys.* **2012**, *14*, 415–426.
- (36) Sasnal, D. K.; Mondal, T.; Mojumdar, S. S.; Choudhury, A.; Banerjee, R.; Bhattacharyya, K. *J. Phys. Chem. B* **2011**, *115*, 13075–13083.
- (37) Mojumdar, S. S.; Chowdhury, R.; Chattoraj, S.; Bhattacharyya, K. *J. Phys. Chem. B* **2012**, *116*, 12189–12198.
- (38) Guzzi, R.; Rizzuti, B.; Bartucci, R. *J. Phys. Chem. B* **2012**, *116*, 11608–11615.
- (39) Hamada, D.; Dobson, C. M. *Protein Sci.* **2002**, *11*, 2417–2426.
- (40) Giurleo, J. T.; He, X.; Talaga, D. S. *J. Mol. Biol.* **2008**, *381*, 1332–1348.
- (41) van den Akker, C. C.; Engel, M. F. M.; Velikov, K. P.; Bonn, M.; Koenderink, G. H. *J. Am. Chem. Soc.* **2011**, *133*, 18030–18033.
- (42) Whitmore, L.; Wallace, B. *Nucleic Acids Res.* **2004**, *32*, W668–W673.
- (43) Taulier, N.; Chalikian, T. V. *J. Mol. Biol.* **2001**, *314*, 873–889.
- (44) Blanco, F. J.; Rivas, G.; Serrano, L. *Nat. Struct. Biol.* **1994**, *1*, 584–590.
- (45) Hamada, D.; Segawa, S.; Goto, Y. *Nat. Struct. Biol.* **1996**, *3*, 868–873.
- (46) Nishikawa, K.; Noguchi, T. *Methods Enzymol.* **1991**, *202*, 31–44.
- (47) Wilson, D.; Valluzzi, R.; Kaplan, D. *Biophys. J.* **2000**, *78*, 2690–2701.
- (48) Kalaiyarasi, M. M.Sc. Thesis, Bharathiar University, Coimbatore, India, 2012.
- (49) Piazza, R.; Lacopini, S. *Eur. Phys. J.* **2002**, *7*, 45–48.
- (50) Gottschalk, M.; Nilsson, H.; Roos, H.; Halle, B. *Protein Sci.* **2003**, *12*, 2404–2411.
- (51) Mendieta, J.; Folqué, H.; Tauler, R. *Biophys. J.* **1999**, *76*, 451–457.